The western termination of the SEMP Fault (eastern Alps) and its bearing on the exhumation of the Tauern Window

Claudio L. Rosenberg and Susanne Schneider

Geological Society, London, Special Publications 2008; v. 298; p. 197-218
doi:10.1144/SP298.10

The western termination of the SEMP Fault (eastern Alps) and its bearing on the exhumation of the Tauern Window

CLAUDIO L. ROSENBERG & SUSANNE SCHNEIDER

Freie Universität Berlin, Institut für Geologie, Malteserstr. 74–100, 12249 Berlin Germany (e-mail: cla@zedat.fu-berlin.de)

Abstract: The SEMP (Salzach–Ennstal–Mariazell–Puchberg) Fault strikes along more than 300 km from the southern margin of the Vienna Basin to the northern Tauern Window accommodating a sinistral displacement of 60 km during Tertiary time. We present new structural data, showing that the SEMP Fault continues into the Tauern Window within a 50 km long mylonitic belt of approximately 2 km width, which we term the Ahorn shear zone. This sinistral shear zone, which marks the northern boundary of the Zentral Gneiss, strikes E to ENE, dips subvertically, and is characterized by gently W-dipping to subhorizontal stretching lineations. S-side-up kinematic indicators in the Y–Z fabric plane and a pronounced southward increase in the inferred temperature of sinistral shearing are observed within the shear zone. Microstructural observations indicate that deformation of quartz at the northernmost boundary of the Zentral Gneiss occurred by dislocation glide with only incipient dynamic recrystallization, suggesting a temperature of approximately 300 °C. Further south, temperatures greater than 300 °C are inferred because all samples are affected by dynamic recrystallization of quartz, and dynamic recrystallization of feldspars also occurred in the southernmost part of the shear zone. These findings point to transpressive deformation accommodating a significant component of south-side-up displacement in addition to sinistral shearing. The sinistral mylonitic foliation forms the axial-plane foliation of the large-scale, ENE-striking upright folds of the western Tauern Window. From east to west, deformation becomes increasingly distributed, passing from an area of interconnected shear zones in the east to a homogeneously deformed mylonitic belt in the west, which terminates into a belt of WNW-striking, upright folds. From the above, we suggest the following: (1) the SEMP Fault extended beyond the brittle-ductile transition to a depth where temperatures exceeded 500 °C (>20 km depth?). These mylonites should be included in the seismic interpretation profiles as a major crustal discontinuity; (2) the large-amplitude, upright folds of the Tauern Window formed at the same time as the sinistral mylonites, and hence during south-side-up differential displacement; and (3) part of the 60 km lateral displacement of the SEMP fault is transferred into a vertical displacement at the western end of the Ahorn shear zone and into a fold belt accommodating NNE-oriented shortening, west of the Ahorn shear zone.

The Tauern Window represents a large (160 × 30 km) exposure of intensively folded lower (European) Plate of the Tertiary Alpine orogeny (Fig. 1c) in the eastern Alps. The uplift and exhumation of this deep structural level occurred mainly in the Miocene, at a time in which the remaining parts of the presently exposed eastern Alps had already been exhumed to a structural level close to the surface. The differential exhumation of this axial zone of the eastern Alps throughout the Miocene was largely accommodated by a series of faults and shear zones bounding the Tauern Window (Fig. 1a, b). These comprise the extensional Brenner and Katschberg faults, marking the western and eastern boundaries of the window respectively, and the Mölltal and SEMP faults, marking the south-eastern and northern boundaries of the window, respectively (Fig. 1a, b). The present paper investigates the structure of the SEMP fault along and across its strike direction and also the relationship between this fault and the internal deformation and exhumation of the Tauern Window.

The SEMP (Salzach–Ennstal–Mariazell–Puchberg) Fault (Ratschbacher *et al.* 1991; Decker *et al.* 1994) strikes along more than 300 km from the southern margin of the Vienna Basin to the northern Tauern Window (Fig. 1a), accommodating a sinistral displacement of 60 km (Linzer *et al.* 1997, 2002) during Tertiary time. Strike-slip deformation along the Inntal Fault (Fig. 1a) is inferred to have been active since the Late Rupelian based on dated sediments deposited along the paleo-Inntal Fault (Ortner & Stingl 2001; Ortner *et al.* 2003). Considering that the SEMP and the Inntal Faults belong to the same sinistral system, which disrupted the North Calcareous Alps into lozenge-shaped blocks during the Tertiary (Frisch *et al.* 1998), one could argue by analogy that the activity of the SEMP Fault also started in the Oligocene. The sinistral DAV Fault (Fig. 1b), marking the southern border of the Tauern Window, is also inferred to be Oligocene in age (Mancktelow *et al.* 2001), and according to some authors it continued to be active during the Miocene (Wagner *et al.* 2006).

From: SIEGESMUND, S., FÜGENSCHUH, B. & FROITZHEIM, N. (eds) *Tectonic Aspects of the Alpine-Dinaride-Carpathian System.* Geological Society, London, Special Publications, **298**, 197–218.
DOI: 10.1144/SP298.10 0305-8719/08/$15.00

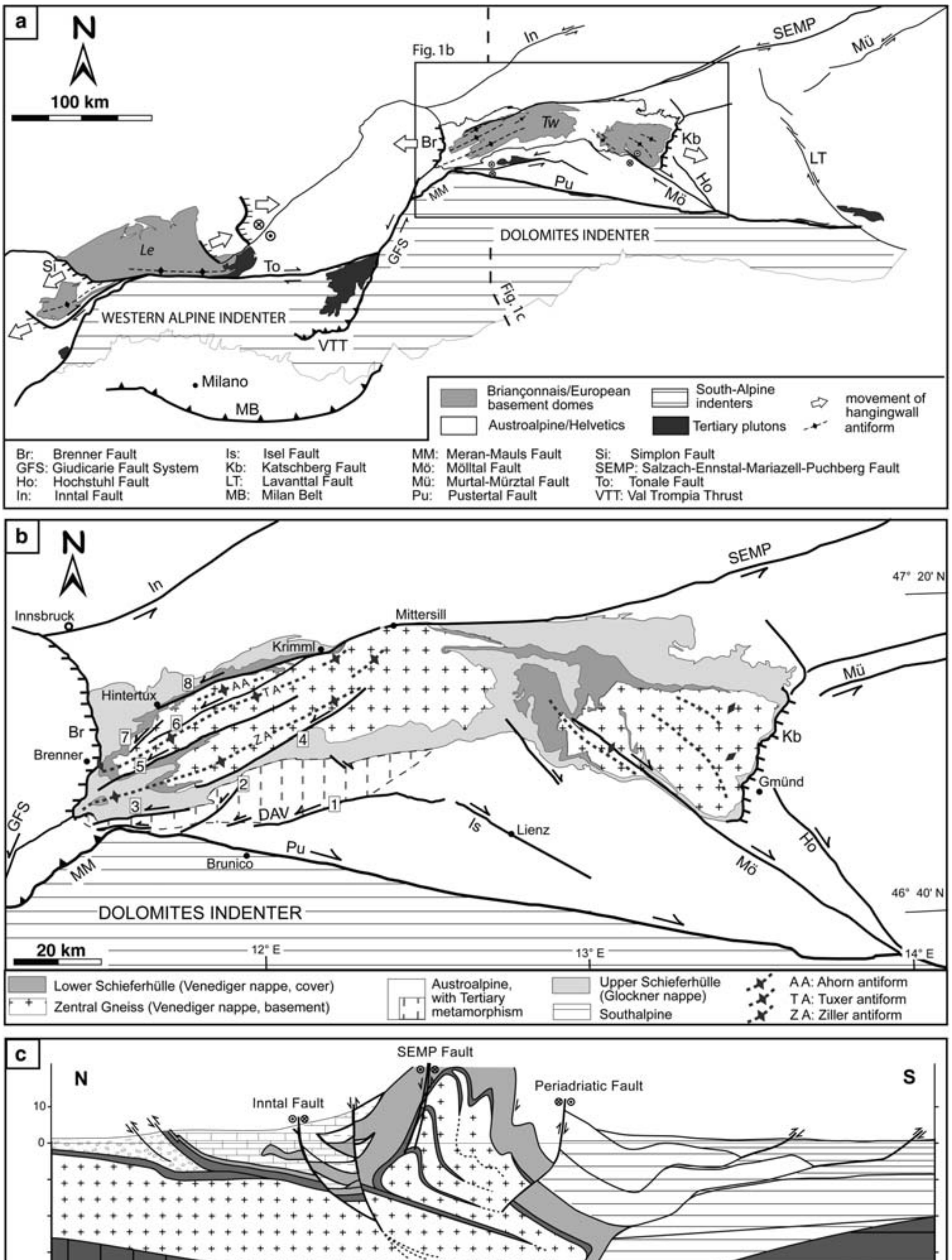

Fig. 1. Tectonic maps and cross-section of the eastern Alps. (**a**) Simplified tectonic map of the Alps, after Handy *et al.* (2005), showing the major Tertiary fault systems. *Le*, Lepontine dome; *Tw*, Tauern Window. Stippled line

In addition, earthquakes recorded throughout the 20th century show a concentration of seismic activity along a linear structure, which roughly corresponds to the fault trace of the SEMP (Reinecker & Lehnhardt 1999; their Fig. 2), suggesting that this fault system may still be active today.

The amount of sinistral displacement and the location of individual fault segments of the SEMP are soundly constrained in the North Calcareous Alps (e.g. Linzer *et al.* 2002), whereas the western termination of this fault in the Tauern Window is not well known. The SEMP Fault becomes ductile as it enters the Tauern Window (Wang & Neubauer 1998), close to Mittersill (Fig. 1). Further west, it was suggested that the SEMP Fault splays into three distinct shear zones (Linzer *et al.* 2002): the Ahrntal Fault in the South (No. 4 in Fig. 1b), the Greiner shear zone (No. 5 in Fig. 1) in the central part of the Zentral Gneiss, and a third shear zone (No. 8 in Fig. 1) at the northern margin of the Zentral Gneiss (Fig. 1). We term this shear zone the Ahorn shear zone, because it affects most of the 'Ahorn Kern' (Ahorn antiform of Zentral Gneiss, Fig. 1b). As shown in Figure 1b, at least two more sinistral shear zones subparallel to the latter three have been mapped in the western Tauern Window (Lammerer & Weger 1998; Mancktelow *et al.* 2001; Kurz *et al.* 2001). Taken together, these closely spaced sinistral shear zones, which strike parallel to upright antiforms, show an 'en-echelon' structure in which the western termination of each shear zone is progressively displaced eastward from south to north (Fig. 1b), except for the Ahrntal Fault (no. 4 in Fig. 1b), whose western termination is however not well known yet. This geometry suggests that the entire western Tauern Window represents a large-scale zone of sinistral, transpressive displacements. Each of these sinistral fault segments is discussed in more detail below.

Sinistral shearing along the Greiner shear zone (Behrmann 1988, 1990) was suggested to be Cretaceous or Eocene, because quartz microstructures in these mylonites were inferred to be statically annealed during the peak of regional metamorphism (30 Ma; Christensen *et al.* 1994) of the Tauern Window (Behrmann & Frisch 1990). In addition, dextral shear zones overprinting the Greiner shear zone were inferred to be *c.* 28 Ma old, suggesting that sinistral shearing must be older than 28 Ma (Barnes *et al.* 2004).

The Ahrntal Fault shows an apparent sinistral displacement of the Zentral Gneiss margin in map view (Fig. 1b). Except for one study, however, in which outcrop-scale kinematic indicators were described from a single locality of the Ahrntal Fault (Reicherter *et al.* 1993), no structural or geochronological investigations of this shear zone exist yet. The spatial continuity between this shear zone and the SEMP Fault is questionable, because a continuous zone of steeply dipping foliations does not occur between the Ahrntal Fault (no. 4 in Fig. 1b) and Mittersill (Fig. 1b), i.e. the northern boundary of the Zentral Gneiss.

The Ahorn shear zone (no. 8 in Fig. 1b) also lacks any structural and geochronological investigations. It strikes subparallel to, and in direct continuation of, the latter, hence being the most obvious continuation of the SEMP Fault within the Tauern Window. A structural and microstructural investigation of this shear zone is the prime subject of the present work.

In the following, we present new structural and microstructural data, which allow us to constrain: (1) the kinematics of the SEMP Fault at deep structural levels; (2) the relationship between this fault and the Brenner fault; (3) the significance of the western termination of the SEMP fault for the exhumation of the Tauern Window; and (4) the anatomy of an orogen-scale strike-slip fault system from a deep-seated structural level, to the upper, brittle crust.

The 'Ahorn' shear zone

The existence of a sinistral shear zone overprinting the northwestern margin of the Zentral Gneiss has been inferred in previous studies. Wang & Neubauer (1998) showed that the SEMP Fault passes into the ductile field in the area west of Mittersill (Fig. 1b). Lammerer & Weger (1988; their Fig. 3a) mapped a sinistral fault along the northwestern margin of the Tuxer Antiform (no. 7 in Fig. 1b). Linzer *et al.* (2002; their Fig. 1) extended the latter fault eastward, along the

Fig. 1. (*Continued*) indicates the trace of cross-section of Fig. 1c. (**b**) Simplified tectonic map of the Tauern Window and surrounding areas. Modified from Rosenberg *et al.* 2007. Fault-name abbreviations are as in Fig. 1a. Numbers indicate the references below, used to compile sinistral faults in the western Tauern Window. 1, Borsi *et al.* (1978); Kleinschrodt (1987); 2, Mancktelow *et al.* (2001); 3, Kurz *et al.* (2001); Mancktelow *et al.* (2001); 4, Linzer *et al.* (2002); 5, Behrmann (1988); Barnes *et al.* (2004); 6, Lammerer & Weger (1998), 7, Lammerer & Weger (1998); 8, Linzer *et al.* (2002) and own work (Fig. 2). (**c**) N–S cross-section of the Alps, striking through the western Tauern Window (stippled line in Fig. 1a), based on surface and seismic data (TRANSALP Line). Modified from Schmid *et al.* (2004). The SEMP Fault is missing in the original cross-section.

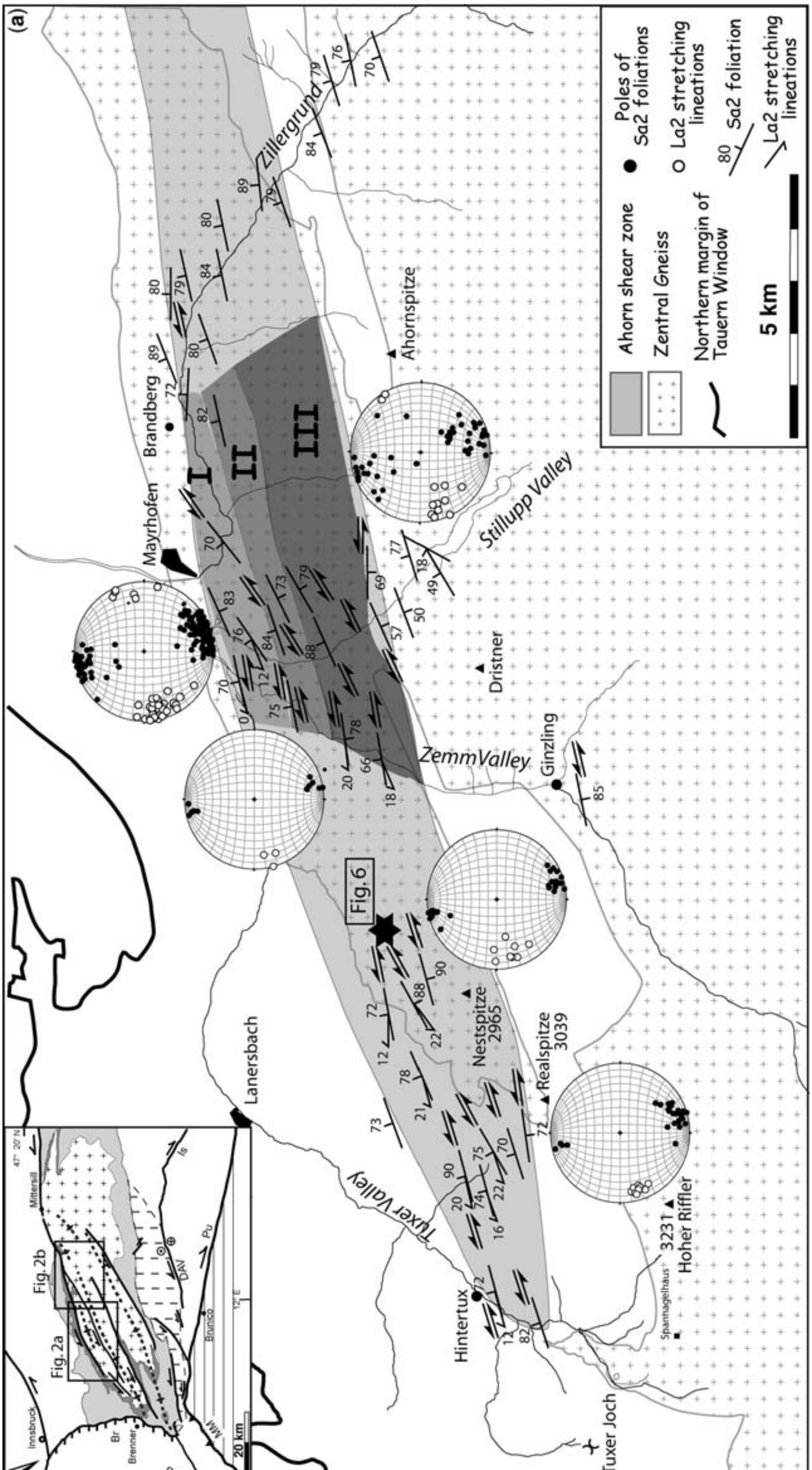
(a)
Zillergrund
Mayrhofen
Brandberg
Ahornspitze
Stillupp Valley
Dristner
Ginzling
Zemm Valley
Fig. 6
Lanersbach
Nestspitze
2965
Realspitze
3039
Tuxer Valley
Hintertux
3231
Hoher Riffler
Spannagelhaus
Tuxer Joch
I
II
III
Ahorn shear zone
Zentral Gneiss
Northern margin of Tauern Window
Poles of Sa2 foliations
La2 stretching lineations
Sa2 foliation
La2 stretching lineations
5 km
Fig.2a
Fig.2b
Innsbruck
Brenner
Br
Mittersill
Brunico
DAV
Pu
Is
GFS
MM
20 km
12° E
47° 20' N

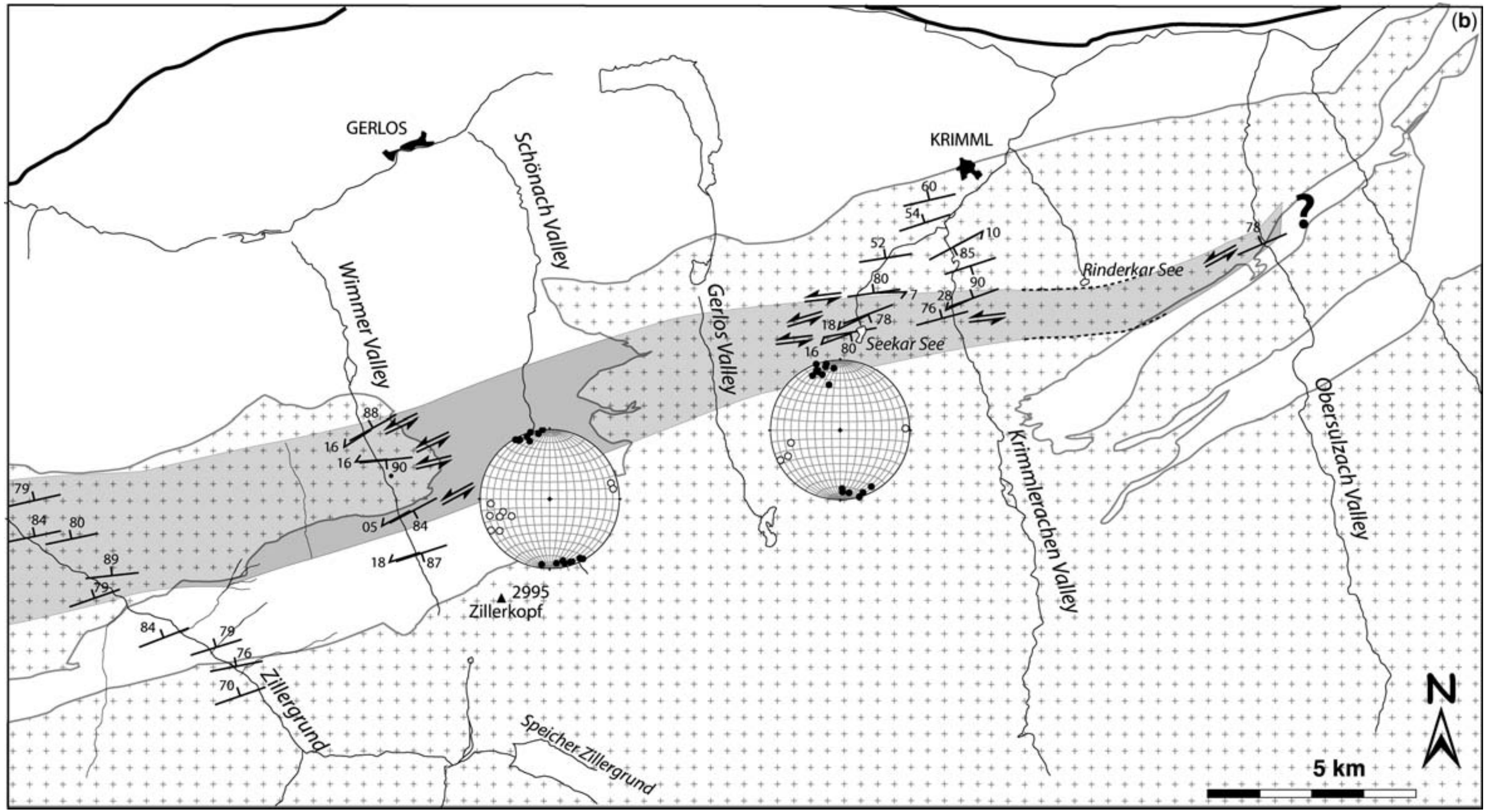

Fig. 2. Structures and location of the Ahorn shear zone. Stereoplots are lower hemisphere projections. The northern margin of the Zentral Gneiss is taken from the geological maps of the Geologische Bundesanstalt (in press), numbers 149, 150 and 151. Note the southward-directed transition from northward dip to southward dip within the Ahorn shear zone. (**a**) Western part of the Ahorn shear zone. The area of the Stillupp and Zemm Valleys is divided into three zones. Zone I is characterized by sinistral mylonites within a biotite-free orthogneiss. Zone III is characterized by sinistral mylonites within an orthogneiss where biotite is stable. Zone II, is intermediate between zone I and zone III. Black star indicates the location of Figure 6. (**b**) Eastern part of the Ahorn shear zone. See Figure 2a for legend. Stippled boundaries indicate the area mapped by Cole *et al.* (2007). Boundaries of the shear zone are taken from their description. Question mark indicates area east of which the Ahorn shear zone has not yet been mapped.

northern margin of the Ahorn antiform (no. 8 in Fig. 1b) to the Salzach Fault, and westward, almost to the Brenner Fault (Fig. 1b). However, no field data supporting the existence of these shear zones and describing the type of deformation in terms of kinematics, microstructures, and inferred deformation temperatures were documented by the latter investigations.

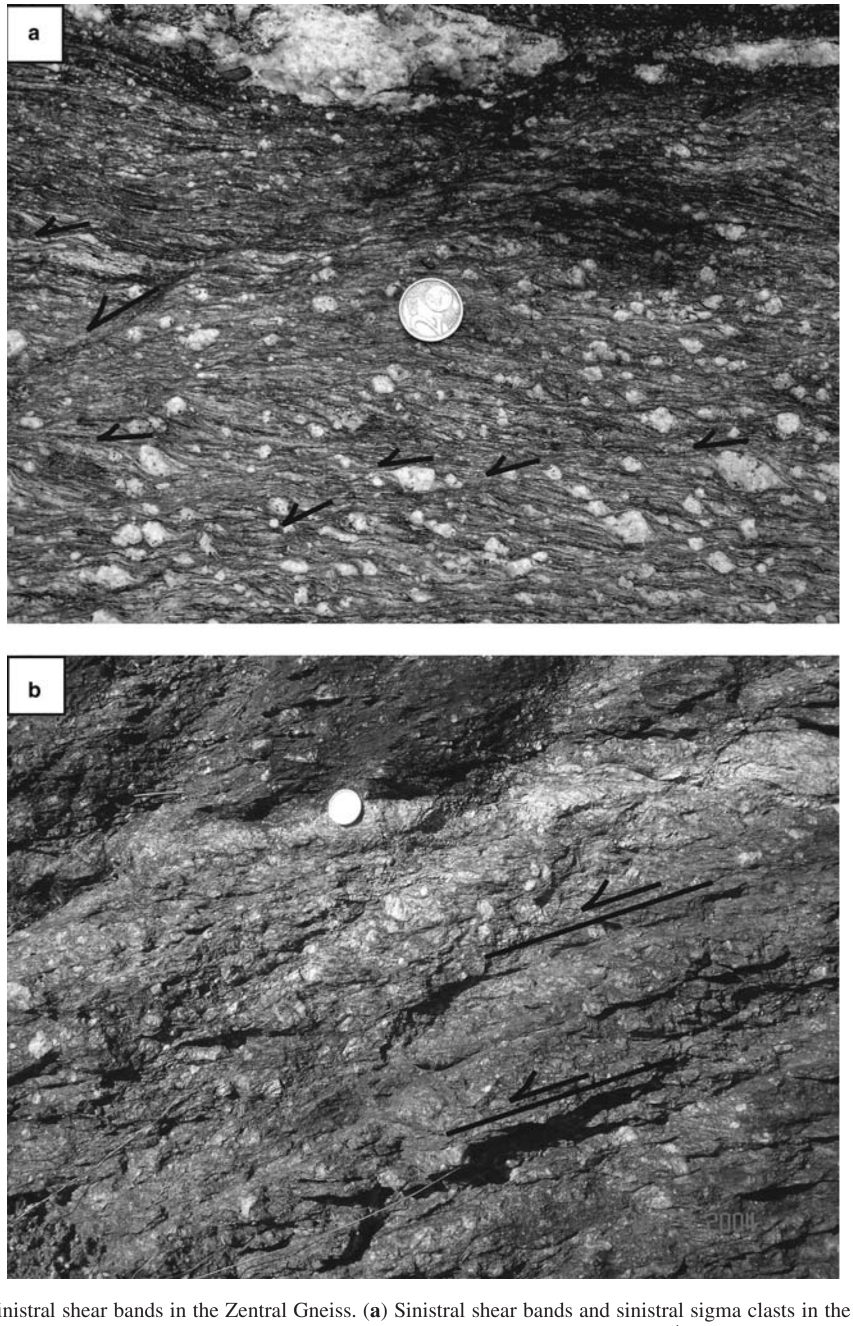

Fig. 3. Sinistral shear bands in the Zentral Gneiss. (**a**) Sinistral shear bands and sinistral sigma clasts in the Sa2 foliation of the Ahorn Orthogneiss from area II (Fig. 2a) (Zemm Valley). (**b**) Discrete C-C′ structures, from the northern most margin of the Ahorn Kern (area I in Fig. 2), Zemm Valley, 1 km north of Figure 3a.

Figure 2 shows the location of the Ahorn shear zone based on our structural mapping. The criterion used to delimit the shear zone was the occurrence of a steeply dipping mylonitic foliation (Sa2), overprinting the main Alpine foliation (Sa1) and pervasively associated with sinistral kinematic indicators (Fig. 3a, b). This second Alpine foliation is rarely observed in the western Tauern Window, outside of this shear zone. As summarized in Table 1, the Sa1 schistosity is generally interpreted to have formed during Early Tertiary, N-directed nappe stacking, and the Sa2 schistosity, during (Miocene?) upright folding.

The Ahorn shear zone has an average width of nearly 2 km, and strikes along the northern margin of the Zentral Gneiss, between Hintertux in the west and Mittersill in the east (Fig. 1). In some areas, the shear zone affects both the Zentral Gneiss and the neighbouring schists of the Schieferhülle, as observed west of the Zemmtal (Fig. 2a). In other areas, as to the south of Krimml (Fig. 2b), the shear zone crosscuts the Zentral Gneiss, without overprinting its northernmost border. Close to its western termination, the shear zone abandons the northern border of the Zentral Gneiss and enters into the Schieferhülle, where its width rapidly decreases in the area of Tuxertal (Fig. 2a), before terminating approximately 2 km south of Hintertux (Figs 1b, 2a). This is indicated by the disappearance of the wide mylonitic belt with its Sa2 mylonitic foliation.

To the west of the shear zone termination (Fig. 2a), sinistral shear senses on E- to NE-striking foliations are not uncommon and generally occur where the S1 foliation is locally rotated into a subvertical orientation. In these outcrops, it is difficult to distinguish whether the foliation is an Sa1 or Sa2, or alternatively a composite foliation. However, the widespread and continuous occurrence of Sa2 foliations clearly ceases west of Hintertux and the main structural grain is formed by Sa1 foliations folded by the upright F2 folds. At its eastern end, the Ahorn shear zone appears to be continuous with and subparallel to the SEMP Fault, suggesting that they are part of one and the same structure.

Structure of the shear zone and relationship to its country rocks

Internal structure

Profiles across the shear zone west of Krimml (Figs 1b, 2b) show a similar structural trend. The Sa2 mylonitic foliation systematically strikes ENE, but the dip direction changes across the shear zone. Foliations dip steeply to the NNW at the northern margin of the shear zone, they become vertical further south, and finally steeply SSE-dipping at the southern margin of the shear zone (Fig. 2a). In contrast, lineations systematically plunge to the WSW with angles varying between 0–25°. Kinematic indicators in the form of pervasive C′ shear bands, indicating a sinistral shear sense are very common.

The average axial ratio of feldspar clasts in the X–Z plane of the deformation ellipsoid progressively increases from north to south (Fig. 4). However, strain analyses performed on the mylonitic augengneiss by the 'Fry' analysis (Fry 1979) on feldspar clasts do not show a strain gradient across the shear zone (Fig. 4). Therefore, the increase in the axial ratio of feldspars is interpreted to be the result of a temperature gradient. In the north of the shear zone, the temperature of deformation was not sufficient to allow the intracrystalline plastic deformation of feldspar, whereas in the southern part of the shear zone this temperature was attained. Based on a review of a large number of natural investigations, Fitz Gerald & Stünitz (1993) showed that the minimum temperature needed for the dynamic recrystallization of feldspar is higher than 450 °C and generally even higher than 500 °C, unless recrystallization occurs by nucleation of new grains and migration of their boundaries. In addition, feldspar ductility (qualitatively expressed by the increase in the axial ratio of feldspar aggregates) increases with increasing temperature (Rosenberg & Stünitz 2003).

In areas dominated by the same lithology, e.g. the porphyritic facies of the Zentral Gneiss as in the Zemmtal or Stilluptal (Fig. 2a), a comparison between Sa2 fabrics across the shear zone shows that the style of the pervasive C′ planes, changes from north to south. These planes are more sharply defined in the north (Fig. 3b), where they look like brittle-ductile structures. Further south, they are characterized by larger widths (Fig. 3a), suggesting a less-localized displacement, as expected for higher temperature conditions.

Relationship between sinistral shearing and upright folding

The structural evolution across the shear zone is similar in all investigated sections. Below, we describe this evolution from south to north.

South of the Ahorn shear zone (Fig. 2), the Zentral Gneiss was affected by two phases of folding. F1 folds are tight to isoclinal, generally recumbent (Fig. 5a–c), with an axial plane schistosity, which forms the main foliation of the western Tauern Window. The axial plane schistosity of F1 represents the first Alpine schistosity (Sa1) in the Zentral Gneiss as previously suggested by most structural investigations in the Tauern Window (e.g. Lammerer & Weger 1998; Table 1).

Table 1. *Compilation of inferred deformation phases in the Tauern Window. Terminology is as found in the literature*

Phase	Structures and tectonic significance	Fabric	Metamorphism/age
	Norris *et al.* 1971		
$\mathbf{F_v}$	Folding with subhorizontal axes		Pre-alpine.
$\mathbf{F_A^1}$	Subisoclinal folds in the Peripheral Schieferhülle. More open folds in the Inner Schieferhülle. Fold axes subparallel to $\mathbf{F_v}$. NE-directed tectonic transport. During late stages of $\mathbf{F_A^1}$ and after F_A^1 formation of Hochalm antiform and Reisseck synform.		Alpine
	Steepening of W-limb of Hochalm antiform between $\mathbf{F_A^1}$ and after $\mathbf{F_A^2}$		Alpine
$\mathbf{F_A^2}$	Flexures, joints and faults, related to vertical movements.		Alpine
	De Vecchi & Baggio 1982		
I	Thrusting and formation of the Vizze syncline (Greiner Zone)		Upper Cretaceous
II	Initial thrusting of the Glockner nappes		Tauern Crystallization. Paleocene-Eocene
III	Final thrusting of the Glockner nappes		Tauern Crystallization. Eocene-Lower Oligocene
IV	Upright folding and uplift of the Tuxer block with respect to the southern part of the Tauern Window	Retrograde metamorphism	Upper Oligocene-Miocene
	Miller *et al.* 1984		
F1	Folding related to nappe stacking	S1 parallel to bedding	Alpine
F2	Local and minor refolding, with N–S striking fold axes.	No schistosity	
F3	Prominent upright folding	No schistosity	
F4	Minor backthrusting	No schistosity	
	Selverstone 1985		
F1	Folding related to formation of nappes with extensive shearing of fold limbs	S1	**USH:** synkinematic growth of porphyro-blasts (grt and Pl) started during F1.
F2	Refolding of previous folds and associated nappes. Upright folds.	Local formation of S2 by crenulation of Bt and Phe.	**LSH:** growth of porphyro-blasts post-dates F1 and is more or less static.
	Lammerer 1988		
D1	Thrusting of Austroalpine on top of Penninc. Top to the N.		Eocene
D2	Isoclinal recumbent folds, involving the uppermost Zentral Gneiss.	Intense schistosity and Lstr., at high angle to fold axes.	
D3	Upright to S-dipping Tux and Zillertal antiforms		
D4	Differential uplift of TW along the Salzach fault		
	Behrmann 1990		
D1	Thrusting (possibly towards 330°, see p. 107)	S1 under prograde conditions	Older than 70–55 My
D2	Tectonic significance unclear.	Formation of S2 or intensification of S1. E–W trending Lstr.	Between 70 and 55 My
D3	Upright folding, N–S shortening during E–W extension or extension in all directions. Sinistral shearing (Greiner shear zone, Knuttenalm, DAV and Speikboden).	Local formation of S3	Between 70–55 and 20 Ma
D4	Early Tertiary Extension of the western Tauern dome		Static thermal peak (Tauern Cristallisation) at the end of D3 D4 between 20 and 15 Ma
	Kupferschmied 1993		
D1	Isoclinal recumbent fold with amplitudes of ca. 5 km	S1 generally sub-parallel to lithological boundaries.	'Early' Alpine age.

(*Continued*)

Table 1. *Continued*

Phase	Structures and tectonic significance	Fabric	Metamorphism/age
D2	Large-scale and nearly coaxial (to D1 ?) folds with similar amplitude of D1.	Folding of S1 and formation of S2 in mica-rich rocks.	Alpine
	Inger & Cliff 1994		
D2	F2 folds (Sonnblick antiform and Mallnitz synform).	Folding of S1. Formation of S2	White mica ages of 28–29 Ma.
D3	Extensional unroofing	Brittle-ductile shear bands, down-to-the-SE shear sense	Alpine
	Kurz *et al.* 1996		
	Southheastern TW		
D0	NNE-directed nappe stacking along brittle thrust planes.		
D1	N-directed ductile nappe stacking. Continuous transition from brittle- to ductile nappe stacking between D0 and D1	S1 parallel to the thrust surfaces and L1, S- to SSE-dipping	S1: Hbl + cpx + bio + ep + Ab, suggesting 6 kb and 500°C
D2		S2 and L2 completely obliterate S1. S1 and S2 form a composite foliation.	Epidote-amphibolite facies
D3	Refolding of the nappe pile during exhumation of the Hochalm dome and development of the Sonnblick dome		
	Northeastern TW		
D0	as above		
D0	as above		
D1	as above	Venediger Nappe: S1 is pre-peak metamorphism and overgrown by Ky, Cld, Hbl and wM.	
D2		Subhorizontal S2 and W- to NW-trending L2 obliterate S1 in the Glockner nappe. S1 and S2 form composite foliation.	
	Lammerer & Weger 1998		
D1	Stacking of Ahorn-, Tux-, and Zillertal gneisses.		Early Tertiary (62 Ma)
D2	Formation of Ahorn, Ziller, and Tux upright antiforms		
D3	Strike-slip faults disrupted the folded structure		
	Kurz *et al.* 2001		
D1	Underplating and top-to-the-N stacking	Penetrative S1 and N–S trending Lstr 1.	
			D1 and D2 are separated by the 'Tauern-Crystallization', D2 is locally contemporaneous to Tauern Crystallization.
D2	Emplacement of penninic nappes onto the European foreland	S2 penetrative foliation and W to NW/SE trending stretching lineation L2.	
D3	Formation of the dome structure. Shear localization along the margins of the dome.	S3 and L3 along shear zones, boundng the Tauern domes.	
	Steffen & Selverstone 2006		
F2	Tight, recumbent folds with N or S plunging axes		
F3	Upright, ENE-striking axial planes and shallowly W-dipping fold axes		
	Present Study		
F1	Tight, recumbent folds	Sa1	Early Tertiary
F2	Upright, ENE-striking folds coeval to sinistral shearing along the SEMP and exhumation of the Tauern Dome.	Sa2 foliation in the Ahorn shear zone	Miocene

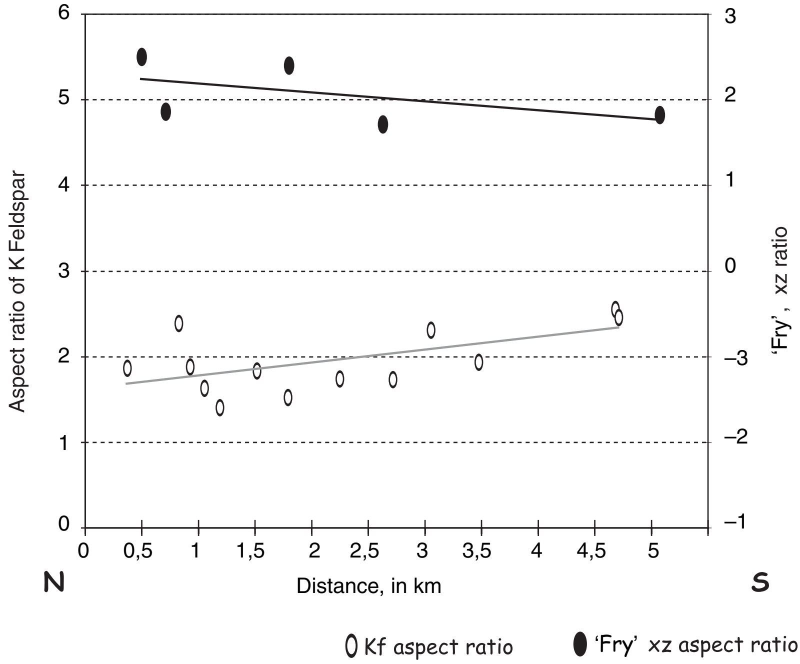

Fig. 4. Axial ratios of feldspars clasts (open ovals) plotted again N–S distance in the Stillupptal (see Fig. 2 for location). Filled ovals: Aspect ratio of deformation ellipses measured in the X–Z section of the inferred deformation ellipsoid on the basis of the Fry analysis. Each aspect ratio is the result of a Fry analysis performed on one sample with 30 to 50 feldspar clasts as centre points.

The F1 folds and the Sa1 foliation are refolded by open to tight F2 folds (Fig. 5a–c), which do not form an axial plane schistosity in this area. Their axial plane is steep to subvertical (Fig. 5b, c) and strikes ENE.

Further north, within the southern part of the Ahorn shear zone (area III in Fig. 2a), F2 folds become tighter and associated with a steeply dipping axial-plane schistosity (Sa2; Fig. 5d) in addition to the folded Sa1. Locally, the folded Sa1 is overprinted by sinistral shear zones, whose length varies from metres to hundreds of metres. These shear zones are sub-parallel to the axial planes of F2.

Still further north within the Ahorn shear zone (area II in Fig. 2a), F1 folds are no longer observed and F2 folds are also very rare. Where found, they occur in the form of dismembered hinges. The Sa2 foliation is very pronounced and it is associated with a pervasive C-C′ fabric (Fig. 3a, b), systematically indicating a sinistral sense of shear. Locally, shear bands and/or shear zones indicating south-side-up displacements (Fig. 5e) also occur within the Y–Z planes, pointing to a transpressive type of deformation. The Sa1 foliation cannot be distinguished anymore because it is completely overprinted by the pervasive Sa2 foliation.

The F2 folds described above (Figs 5b, c and 6a) are parasitic folds of the large-scale, upright, ENE-striking antiforms, which form the structural grain of the western Tauern Window (Fig. 1a, b). The structural sequence described above points to a N-directed increase in the intensity of F2 shortening within our study area, culminating at the northernmost contact of the Zentral Gneiss, which is pervasively overprinted by a mylonitic Sa2 foliation. The parallelism between mylonitic Sa2 schistosity and the axial plane of the F2 folds suggests contemporaneous sinistral shearing and folding in the western Tauern Window. This interpretation is also supported by the direct observation of the Sa2 foliation with associated sinistral kinematic indicators (Fig. 6c), forming the axial plane schistosity of the F2 upright folds of the Ahorn antiform (Fig. 6a).

Microstructural changes across the shear zone

The microstructures of the mylonitic Zentral Gneiss vary across the Ahorn shear zone. We describe them from S to N below.

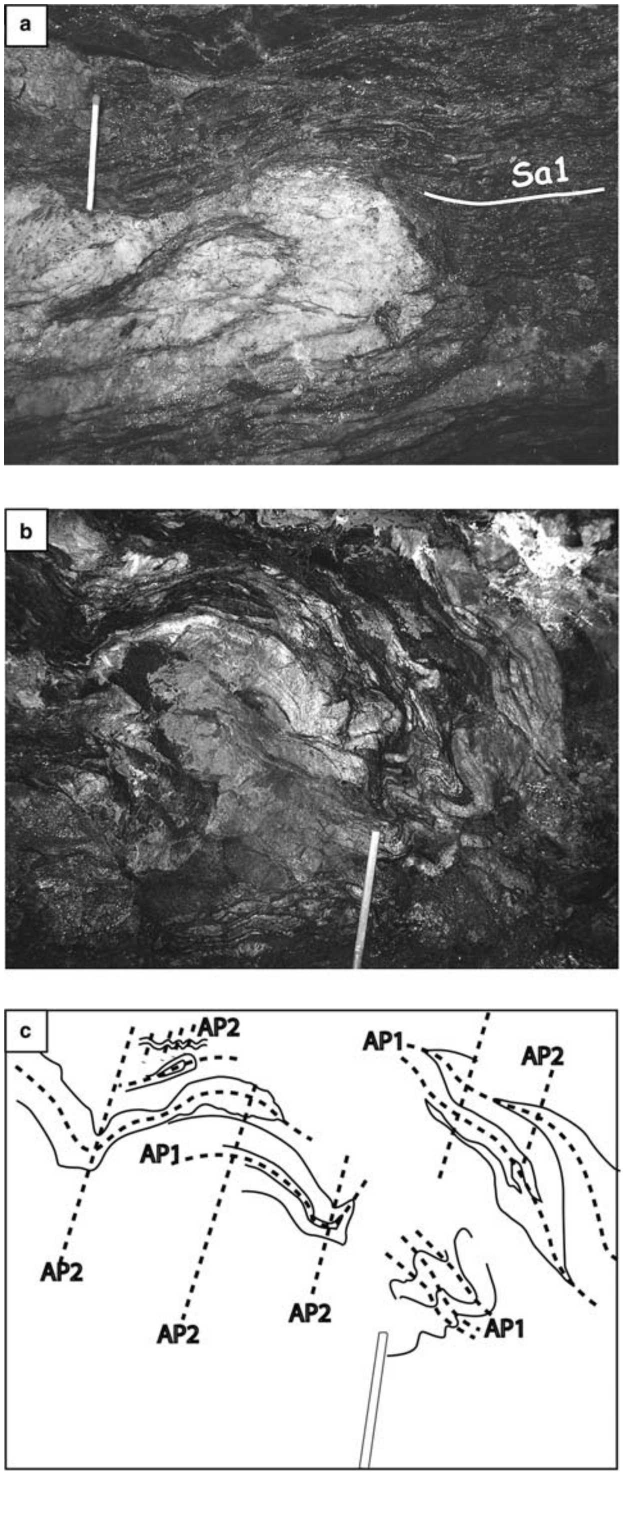

Fig. 5. *Continued.*

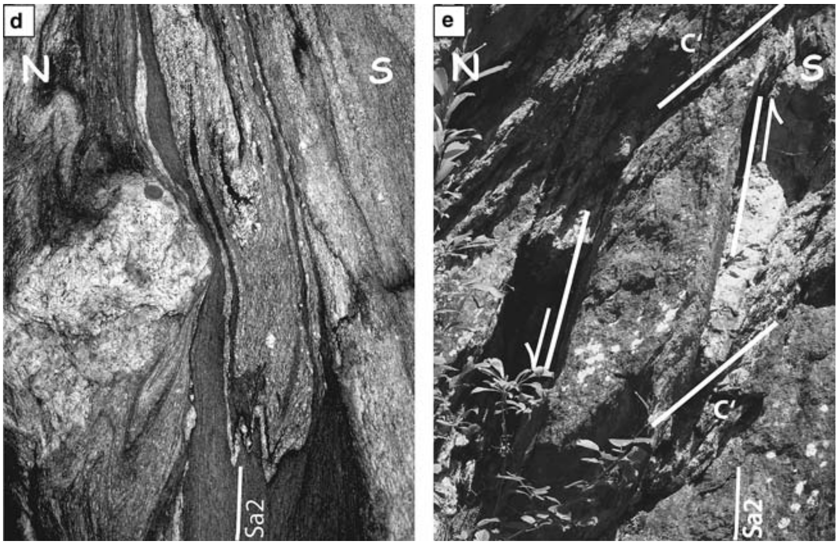

Fig. 5. (*Continued*) Field photographs from the Stillupp and Zemm valleys (Fig. 2). (**a**) Fa1 recumbent folds, within migmatitic gneisses, showing an Sa1 axial plane foliation within the dark, mica-rich layers. Upper Stillupp valley. (**b**) Open, upright Fa2 folds within migmatitic gneisses, refolding Fa1 folds, in the upper Stillupp valley. Hammer of 80 cm length for scale. (**c**) Line drawing of Figure 3c, showing the traces of the axial planes of the first phase (AP 1) and of the second phase (AP 2) of folding. (**d**) Isoclinal, upright Fa2 folds, with pronounced Sa2 axial plane foliation. This foliation is characterized by systematic and pervasively distributed sinistral kinematic indicators (mostly shear bands). Zemm Valley. (**e**) South-side-up shear sense in the Y–Z plane. Stillupp valley. Shorter side of the photographs is 60 cm long.

At the southernmost boundary of the Ahorn shear zone (area III in Fig. 2a), where the Zentral Gneiss is only locally overprinted by the Sa2 foliation within metre-scale sinistral shear zones (Fig. 7a), quartz grains have lobate boundaries (Fig. 7b), with lobe sizes of 50 to 100 μm, indicating recrystallization by grain boundary migration (Regime III of Hirth & Tullis 1992). Feldspars also show new grains with lobate boundaries within elongate tails of feldspar porphyroclasts (Fig. 7b). These observations point to a deformation temperature probably above 450–500 °C (for review, see Fitz Gerald & Stünitz 1993).

Further north (area II in Fig. 2a), the microstructures of quartz and feldspar are significantly different. Quartz grains have lobate grain boundaries (Fig. 7c), but the size of the lobes and of the grains is smaller compared to the samples located southward. No evidence for dynamic recrystallization of feldspar grains is found within these samples. Assuming similar strain-rate conditions between this area and the one described above, these microstructural differences indicate that sinistral shearing in the latter sample occurred under lower temperature conditions. This assumption is reasonable in the light of the distributed character of deformation within all parts of the shear zone.

In the northernmost area (area I in Fig. 2a), quartz grains are more elongate than in the previous samples (Fig. 7e, f), but they are not recrystallized, or only very locally. In contrast, they show strong undulose extinction (Fig. 7e), eventually passing into deformation bands. Where present, recrystallized grains have small sizes (10 to 20 μm) and serrated boundaries, which point to recrystallization by bulge nucleation. Feldspars form competent clasts in these mylonites and their occasional internal deformation only occurs by cataclasis (Fig. 7f) or shearing along retrograded, saussuritic domains. Flame perthites and exsolution to albite and plagioclase are common at the rims of the clasts. Sinistral shearing within these rocks was mainly partitioned into an interconnected weak layer (Handy 1990), consisting of fine-grained aggregates of white mica (Fig. 7e, f), locally containing minor amounts of quartz and albite. These fine-grained aggregates flow around the elongate and partly boudinaged quartz grains (Fig. 7e, f), indicating that quartz was more competent under these temperature conditions. This competence contrast does not persist in the southern part of the shear zone, where deformation is equally partitioned within the quartz and the mica aggregates (Fig. 7c, d). Assuming a similar strain rate as in the samples

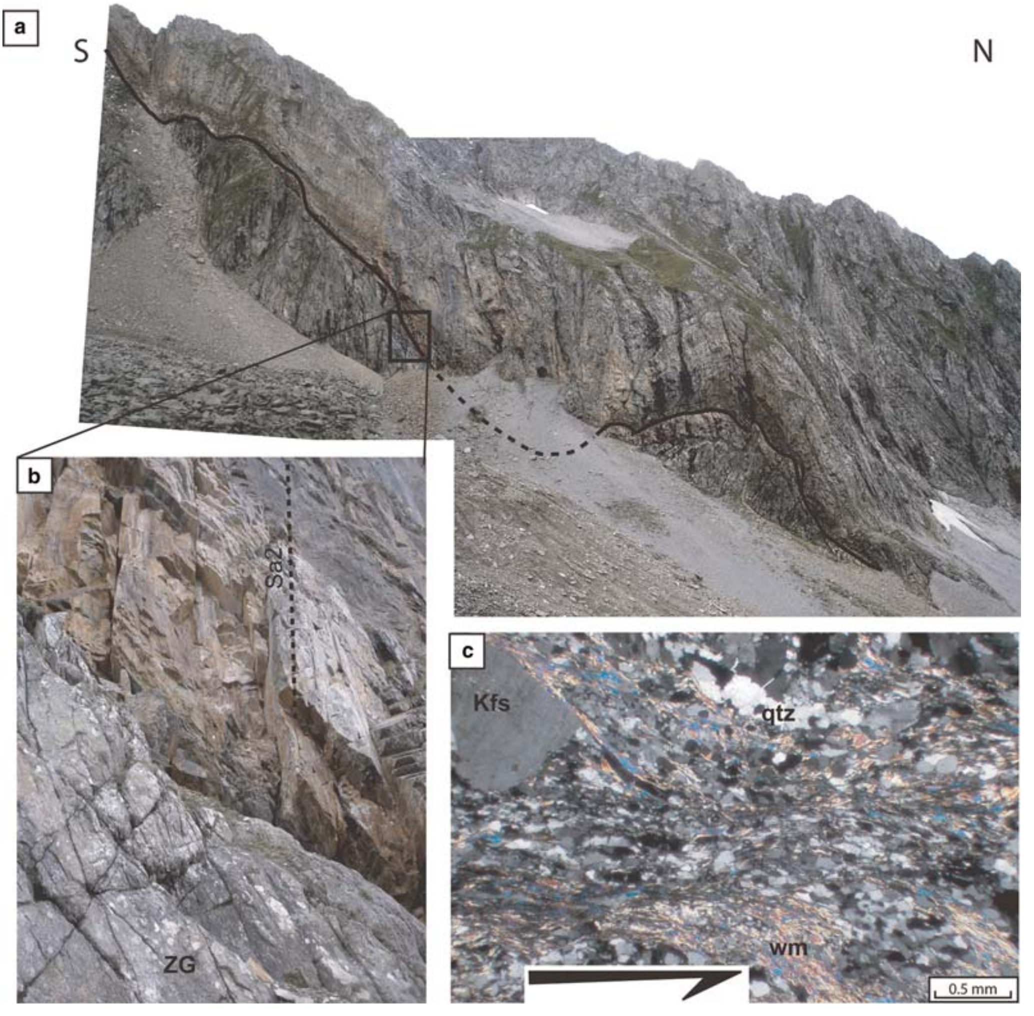

Fig. 6. Structures and microstructural relationship between F2 folding and Sa2 foliation in the Ahorn dome, Inner Elskar (Fig. 2a for location). (**a**) F2-Folded contact of Zentral Gneiss and Schieferhülle on the northern limb of the Ahorn antiform (Fig. 1), Inneres Elskar, Ziller Valley. Black line marks the contact between Zentral Gneiss and Lower Schieferhülle. (**b**) Detail of Figure 6a, showing the axial plane foliation Sa2, cross-cutting the boundary between Zentral Gneiss (below; ZG) and Triassic quartzites above. (**c**) Micrograph, with crossed-polarizers, indicating sinistral shear bands in the Zentral Gneiss sampled in the outcrop of Figure 6b.

of Figure 7(c) and (e), the microstructural difference described above can be attributed to a northward decrease in the temperature of deformation.

The aforementioned microstructural changes go together with a change in the modal composition of the samples. From south to north, the content of biotite progressively decreases, becoming replaced by fine-grained white micas (compare Fig. 7c, e), oxides and/or chlorite within grain fractures. At the northern margin of the Zentral Gneiss, biotite is almost completely absent. These findings support the interpretation of the northward transition of recrystallization mechanisms in terms of a decrease in deformation temperature. The northward decrease in the axial ratio of the feldspar clasts at relatively constant bulk strain (Fig. 4) is also consistent with lower temperatures in the north: the higher axial ratios in the south are likely due to increased feldspar ductility compared with brittle feldspar behaviour in the north.

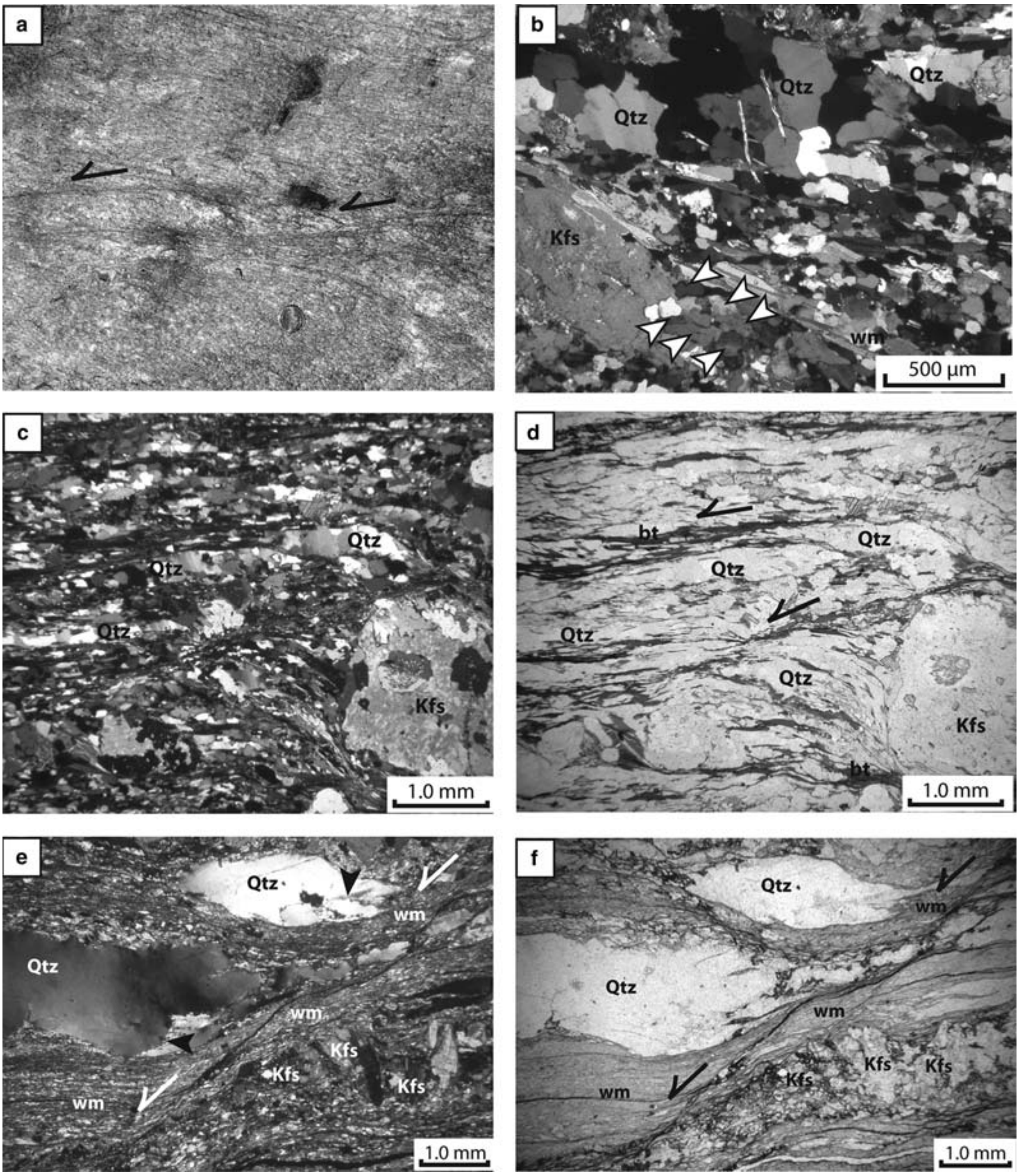

Fig. 7. Structure and microstrucures of Sa2 foliation along a S–N traverse through the Zemmtal. (**a**) High-temperature, sinistral shear zones at the southernmost margin of the Ahorn Shear zone, Zemm Valley. In this area, the mylonitic Sa2 foliation only occurs within discrete, metre-long sinistral shear zones, which overprint the Sa1 foliation. (**b**) Photomicrograph with cross-polarized light showing the microstructures within a shear zone of Figure 7a. Note the large and lobate grains of quartz (qtz) and the recrystallized grains of feldspar (white arrowheads) in the pressure shadow of a larger clast (Kfs). wm: white mica. (**c**) Microphotograph with cross-polarized light. Sa2 foliation from the southern part of the Ahorn shear zone, Zemm Valley. Note the dynamically recrystallized aggregates of quartz. (**d**) Microphotograph with plane light. Same sample as in Figure 7c. Note the localization of deformation into sinistral shear bands, consisting of quartz, white mica and biotite. (**e**) Microphotograph with cross-polarized light. Sa2 foliation from the northernmost part of the Ahorn shear zone, Zemm Valley. Note the elongate and boudinaged quartz grains, with deformation bands and undulose extinction. Recrystallization of quartz is very limited (black arrowheads). (**f**) Microphotograph with plane light. Same sample as in Figure 7e. Note that deformation does not localize into quartz aggregates, but into sinistral shear bands, consisting of very fine-grained white mica.

Structure of the country rocks west of the Ahorn shear zone

The area located immediately west of the termination of the Ahorn mylonitic belt, i.e., west of Hintertux (Figs 1b and 2b) is affected by intense shortening accommodated by upright folds striking WNW–ESE (Fig. 8). These folds fold the Sa1 schistosity and do not form a new axial plane foliation. Therefore, they can probably be attributed to the F2 phase. However, the orientation of the axial planes of these folds differs from that of the F2 axial planes measured further east, which strike WSW–ENE, as do most structures of the western Tauern Window (Fig. 1b). At present, we do not have more data to constrain the northern, southern and western termination of the area characterized by upright folds with WNW-striking axial planes. However, we emphasize the spatial coincidence between the rotation of the F2 axial planes from an ENE to a WNW strike and the termination of the Ahorn shear zone (Fig. 8).

Discussion

Alpine deformation phases and fabrics

The Ahorn shear zone is characterized by a mylonitic Sa2 foliation, which forms the axial plane schistosity of the northernmost upright antiforms of the western Tauern Window, i.e. of the Ahorn antiform (Fig. 1b). This relationship, which points to contemporaneous upright folding and sinistral shearing of the Ahorn core, is in contrast to previous work (Kurz *et al.* 2001), which suggested that deformation in this area pre-dated the formation of the Tauern dome and the formation of shear zones bordering the dome.

The fact that the mylonitic Sa2 foliation is not folded and is axial planar to the F2 upright folds suggests that it formed in a steep orientation, probably similar to the present one (Fig. 2), because no significant deformation phases younger than F2 are observed in this study area (Table 1). A similar structural relationship between sinistral shearing and upright folding has been suggested by Kleinschrodt (1987) and Wagner *et al.* (2006) for the DAV Shear Zone (Fig. 1b), which marks the southern border of the Tauern structural and thermal dome (Frisch *et al.* 2000).

A static recrystallization event associated with the Tertiary metamorphic peak has often been invoked in the Venediger Nappe Complex of the Tauern Window (e.g. Behrmann 1990; Kurz *et al.* 2001). This static event has been interpreted as the result of the 'Tauern crystallization' of Sander (1920), although Sander originally described it as a dynamic metamorphic event. We found no microstructural evidence pointing to static recrystallization in the Ahorn Kern, neither within the Ahorn shear zone nor outside of the shear zone (Fig. 7). Even the high-temperature deformation fabrics of the southern border of the shear zone and the Sa1 fabrics outside of the shear zone (Fig. 9) indicate the preservation of dynamic fabrics characterized by lobate grain boundaries and subgrains within the quartz aggregates. Therefore, both the peak of Tertiary metamorphism and the retrograde metamorphic overprint occurred under dynamic conditions in our study area. Interestingly, Steffen *et al.* (2001) and Steffen & Selverstone (2006) showed that even some apparently 'post-kinematic' Garbenschiefer fabrics south of our study area are syndeformational. This may suggest that the 'Tauern crystallization' was syntectonic throughout the Tauern Window.

Age of folding and sinistral shearing

F2 upright folds were suggested to be late and mainly post-peak of Tertiary metamorphism, i.e. upper Oligocene to Miocene, because the F2 folds fold the isograds of Tertiary metamorphism (de Vecchi and Baggio 1982). Behrmann (1990; Table 1) suggested that F2 folding occurred between 70–55 and 20 Ma. Wagner *et al.* (2006) interpreted the steep orientation of the Austroalpine basement south of the western Tauern Window as due to F2 folding, which was inferred to be Late Oligocene based on cross-cutting relationships with the 30 Ma old Rieserferner intrusion.

In the present study, we showed that the upright folds of the Tauern Window probably formed at the same time as sinistral shearing along the western termination of the SEMP Fault. Therefore, the age of displacement along the SEMP Fault may be used to date F2 folding in the western Tauern Window. Sinistral shearing along the SEMP is inferred to be of Karpatian age (17 Ma; Peresson & Decker 1997) on the base of deformed, dated conglomerates (Steininger *et al.* 1989). The major phase of lateral escape and hence of activity of the SEMP Fault was suggested to be between 23 Ma and 12–13 Ma (Frisch *et al.* 1999). As a consequence, sinistral shearing along the Ahorn shear zone and upright folding in the western Tauern Window may also be lower to Middle Miocene in age. However, Most *et al.* (2003) showed a very pronounced southward younging of apatite fission track ages across the Ahorn shear zone (Fig. 10), from 12 Ma at the northern shear zone boundary to 7 Ma at the southern boundary. Therefore, significant south-side-up displacements were accommodated by the Ahorn shear zone in the upper Miocene. The spatial coincidence of this pronounced age gradient

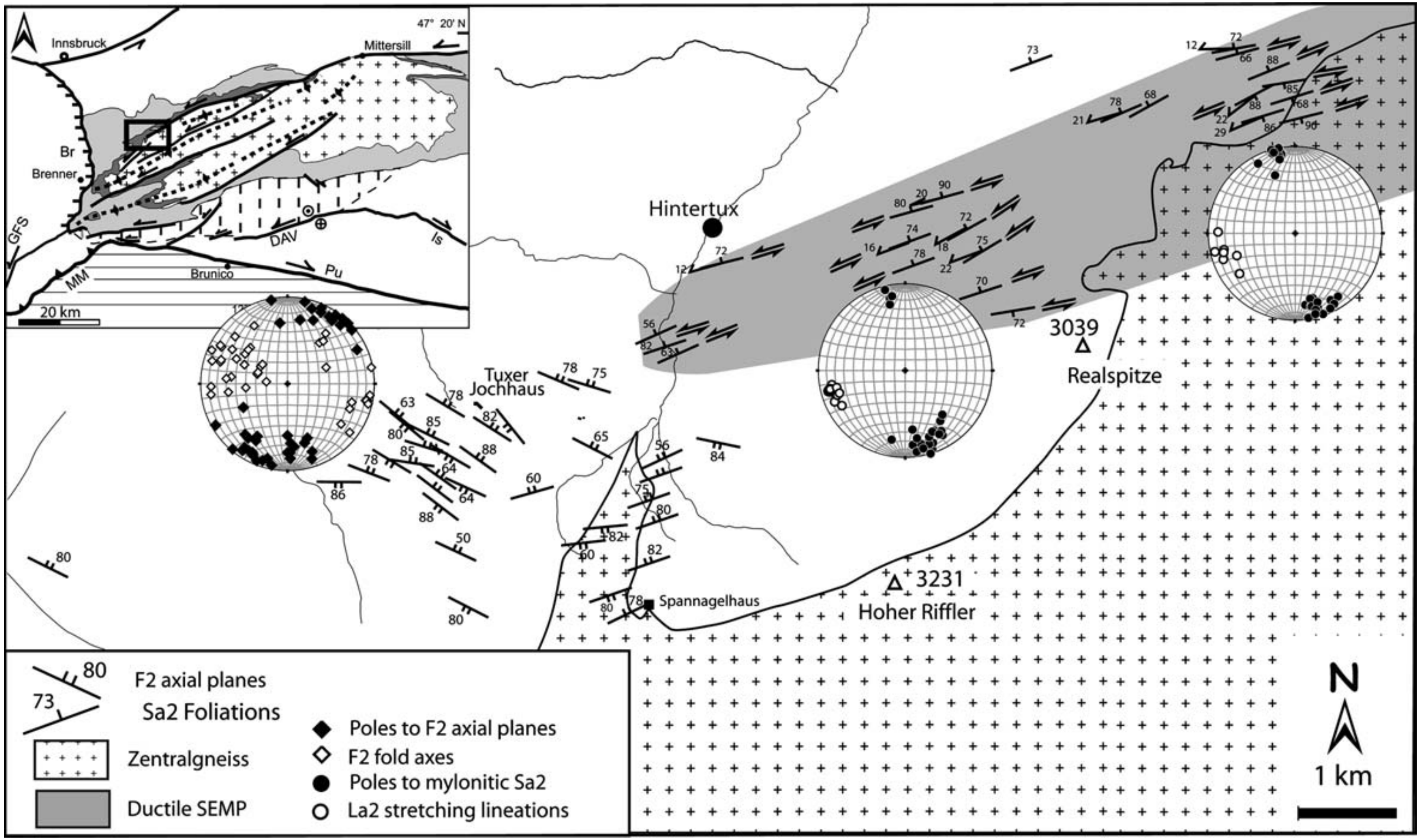

Fig. 8. Structural map, displaying the orientation of F2 axial planes at the western end of the Ahorn shear zone. Note the rotation of F2 axial planes from ENE-striking in the east, to WNW-striking in the west.

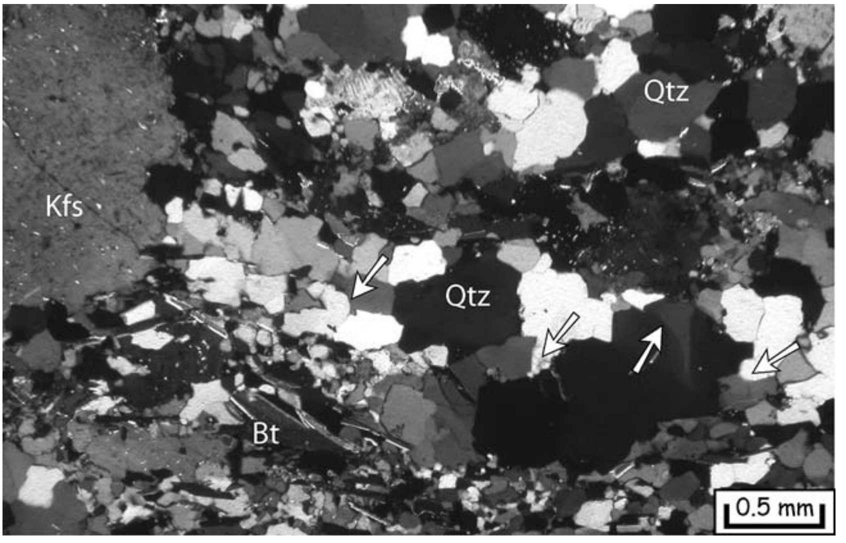

Fig. 9. Microstructures of Sa1 schistosity. White arrows directed to the bottom show large lobate boundaries of quartz grains, indicating dynamic recrystallization by grain boundary migration. White arrow directed to the top shows the occurrence of deformation bands within a quartz grain. These microstructures suggest that this Early Alpine schistosity was not statically annealed.

(Fig. 10) and the location of the transpressive mylonitic belt of the Ahorn shear zone, suggest that the south-side-up displacement indicated by the FT ages of apatites (Most *et al.* 2003) may be contemporaneous with sinistral displacements. In this case, sinistral shearing in the Ahorn shear zone would also have been active until the upper Miocene.

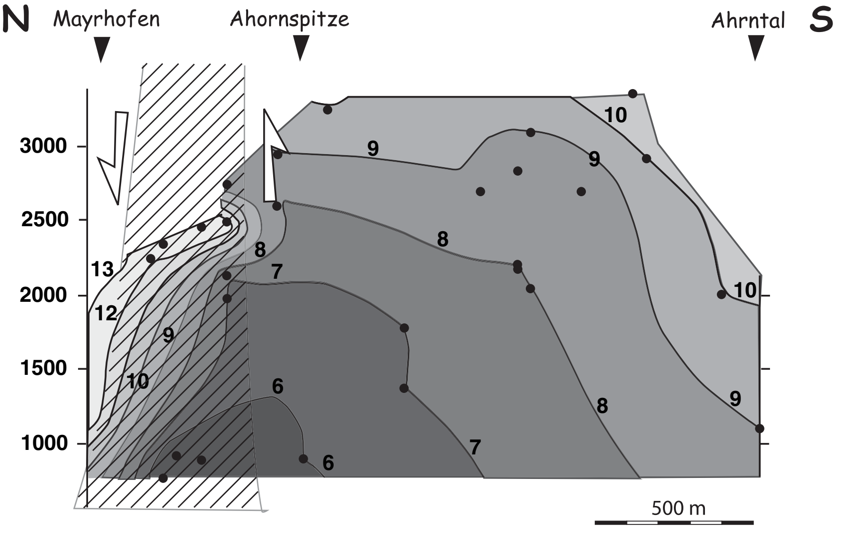

Fig. 10. Fission track apatite ages, modified after Most *et al.* (2003). Note the very rapid younging of fission track ages located exactly along the Ahorn shear zone, indicating a pronounced south-side-up displacement, probably younger than 7 Ma. Numbers on curves are ages in millions of years.

Kinematics of the Ahorn shear zone

The occurrence of a southward increase in the temperature of deformation within the Ahorn shear zone, and the fact that the Ahorn shear zone separates an area with Tertiary amphibolite-facies metamorphism in the south (e.g. Hörnes & Friedrichsen 1978) from an area in the lowest greenschist facies (just above the brittle-ductile transition in quartz) in the north points to a south-side-up component of displacement acting along the shear zone. It is difficult to quantify the absolute temperature difference between the southern and northern margins of the Ahorn shear zone only on the base of quartz recrystallization mechanisms, because the transition temperatures from one mechanism to the other are temperature-, but also strain-rate dependent (Stipp *et al.* 2006). However, a large number of field studies (Fitz Gerald & Stünitz 1993, for a review) suggest that dynamic recrystallization of feldspar initiates at temperatures above 450–500 °C. Therefore, this temperature may be considered as a minimum estimate of the maximum temperature during shearing at the southern margin of the Ahorn shear zone. The lowest temperature of shearing, at the northern margin of the Ahorn shear zone, can be constrained on the basis of quartz grains, showing microstructural evidence for dislocation glide (Fig. 7e), but no evidence for dislocation creep. This transition is inferred to be at temperatures $\geq$280 °C for rocks deforming at strain rates within the commonly inferred range of 10^{-11} s^{-1} to 10^{-14} s^{-1} (Stipp *et al.* 2002).

These temperature estimates point to a difference of approximately 200 °C between the southern and northern boundaries of the Ahorn shear zone, in the area of the Stillupp and Zemm valleys (Fig. 2a). Considering a geotherm of *c.* 30 °C/km in order to describe a simplified crust for illustrative purposes, the aforementioned temperature difference may correspond to a vertical offset of *c.* 7 km. This offset could result from sinistral shearing parallel to the west-plunging stretching lineations (Fig. 2). However, given the transpressive character of the shear zone, the transport direction may have been steeper than the stretching lineation (e.g. Robin & Cruden 1994).

As a consequence, the lateral offset of 60 km, which affected the SEMP Fault east of the Tauern Window (Linzer *et al.* 2002), is partly transferred into a vertical one in the Ahorn shear zone. This conclusion is consistent with the western termination of the shear zone, which is observed to pass into a zone of upright folds, probably accommodating a component of vertical extension.

Kinematic link between the SEMP and the Brenner Faults

The Ahorn shear zone terminates in the area east of the Tuxer Joch (Fig. 2a), approximately 15 km east of the Brenner Fault (Fig. 2). Therefore, in contrast to previous interpretations (Linzer *et al.* 2002), the SEMP Fault and the Brenner Fault are not in spatial continuity, and the Brenner Fault does not form the lateral ramp of the SEMP Fault. The lateral displacement of the Ahorn shear zone passes into a WNW–striking folded structure which accommodates shortening in an approximately NNE–SSW directed orientation (Fig. 11), and not into an E–W directed extension.

The fact that folds with anomalous orientations (WNW-striking axial planes, Fig. 8) occur exactly in the spatial continuation of the Ahorn shear zone termination suggests that the latter structures are genetically related. We envisage that NNE-oriented shortening becomes partitioned into a sinistral displacement within the Ahorn shear zone and a NNW-oriented shortening component to the south of the shear zone (Fig. 11). West of the shear zone termination, NNE-directed shortening is not partitioned into a lateral, sinistral displacement, hence resulting in folds with axial planes approximately perpendicular to the shortening direction. As a consequence, the sinistral displacements of the SEMP Fault and the Ahorn shear zone are transferred into an area of NNE-directed shortening (Fig. 11), not in an E–W extensional deformation.

The other sinistral shear zones previously suggested to be splays of the SEMP Fault (nos. 4 and 5 in Figure 1b; Linzer *et al.* 2002) also lack a kinematic continuity with the Brenner Fault. The spatial relationship between Brenner Fault and Greiner shear zone (no. 5 in Figure 1b) cannot be satisfyingly solved due to the lack of outcrops in the critical area, where overprinting structures would be expected (Behrmann 1988). We note however, that if the Greiner shear zone continued westward until the Brenner Fault without a marked change of strike, it would reach the Brenner Fault at its southern end (Fig. 1b). In this area, the kinematics of the west-dipping Brenner extensional fault would predict a dextral shear zone, associated with exhumation of the footwall of the Brenner Fault (e.g. Fügenschuh *et al.* 1997) and not a sinistral shear zone. Therefore, a direct kinematic link between the Greiner shear zone and the Brenner Fault is unlikely. The same line of arguments precludes a kinematic link between the sinistral Ahrntal Fault (Fig. 1) and the Brenner Fault. The westward continuation of the Ahrntal Fault would also reach the Brenner Fault at its southernmost margin.

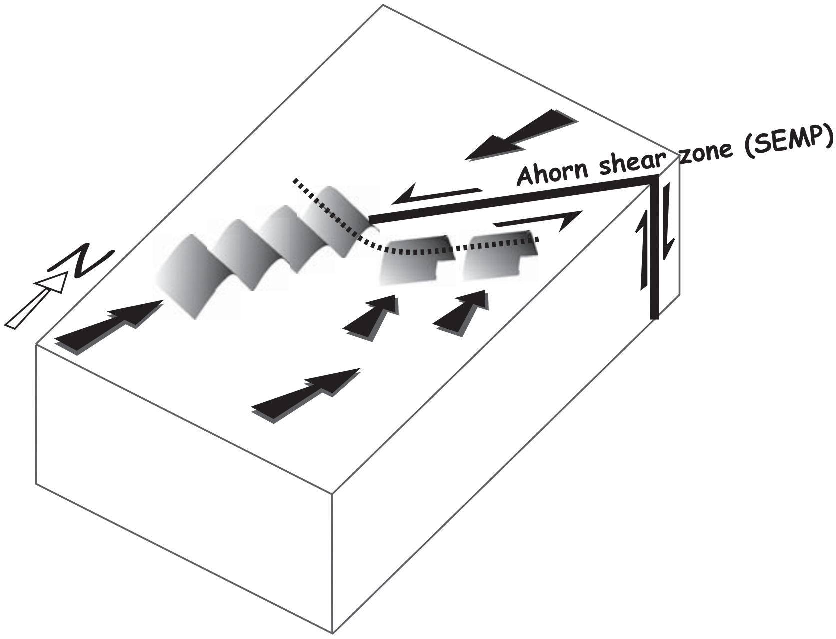

Fig. 11. Schematic block diagram indicating the relationship between inferred direction of shortening and the resulting first order structures at the western termination of the Ahorn shear zone. West of the termination of the Ahorn shear zone, NNE-oriented shortening leads to the formation of WNW-striking axial planes. South of the termination of the Ahorn shear zone, NNE shortening is partitioned into a lateral ENE-striking sinistral shear component and a pure shear component oriented perpendicular to the shear zone, i.e. NNW.

Anatomy of the SEMP Fault from the upper crust to the middle/lower crust

An along-strike, brittle-ductile transition within the SEMP Fault has been described in the area of Mittersill (Wang & Neubauer 1998; Fig. 1). This transition is described within metapelites and carbonatic schists containing calcite mylonites. The brittle-ductile transition in these rocks is controlled by the onset of intracrystalline plastic deformation of micas and calcite, which is constrained to occur at temperatures $<250\,^{\circ}\mathrm{C}$ (e.g. Burkhard 1993), whereas the same transition in the quartz-dominated Zentral Gneiss probably occurred at temperatures $\geq 280\,^{\circ}\mathrm{C}$ as constrained by Stipp *et al.* (2002) for quartz veins in the contact aureole of the Adamello batholith. In the area of Rinderkarsee (Fig. 2b), located approximately 20 km west of Mittersill, Cole *et al.* (2007) described a wide zone (1300 m) of sinistral deformation within the Zentral Gneiss, in which shearing is heterogeneously distributed into individual shear zones. Further west, at Seekarsee (Fig. 2b), sinistral shear zones of tens to hundreds of metres thickness alternate with areas of hundreds of metres thickness where the Zentral Gneiss is largely undeformed, locally preserving its prealpine magmatic fabric. West of Krimml (Figs 1 and 2b), sinistral deformation becomes homogeneously distributed within a zone of approximately 2 km thickness. Undeformed areas within this zone do not occur anymore and the Zentral Gneiss consists everywhere of an S-C type mylonite (Fig. 3).

These changes in the spatial pattern of deformation partitioning are often suggested to characterize the depth-dependent brittle-ductile transition of large-scale faults (e.g. Twiss & Moores 1992). The fact that the microstructures observed in the areas of Zemmtal and Stillupptal (Fig. 7) indicate sinistral shearing at temperatures much higher than those described further east by Cole *et al.* (2007) and Wang & Neubauer (1998) suggests a continuous westward increase in the deformation temperature and hence a deeper exposure level of the SEMP Fault, from Mittersill to Rinderkarsee, and to the Ahorn Kern (Fig. 2). Taken together, these interpretations suggest that the SEMP Fault consists of discrete brittle faults in the upper crust (presently exposed east of Mittersill; Linzer *et al.*

2002) of an anastomozing network of shear zones close to the brittle-ductile transition, as presently exposed south of Krimml (Cole *et al.* 2007), and of a distributed deformation as shown by the structures exposed in the area west of Krimml (Fig. 2a, b). In contrast to Wang & Neubauer (1998), we find no coaxial flattening in the ductile part of the SEMP Fault, and no decrease in the shear zone width with increasing depth.

Conclusions

The SEMP Fault extended beyond the brittle-ductile transition to a depth where temperatures probably exceeded 500 °C (>20 km depth?). The present-day surface exposure of this fault shows a transition from brittle faulting in the east to an area of anastomozing, ductile shear zones and finally to a homogeneously deformed mylonitic belt further west.

The large-amplitude, upright folds of the Tauern Window formed at the same time as the sinistral mylonites during the activity of the SEMP Fault, which may have started in the Oligo(?)-Miocene. Vertical, differential displacements indicated by pronounced younging of apatite and zircon fission track ages (Most *et al*. 2003) exactly across the trace of the Ahorn shear zone, suggest that the shear zone was still active in the uppermost Miocene. Part of the pronounced lateral displacement of the SEMP Fault is transferred into a vertical displacement at its western end, and into NNE-directed shortening, accommodated by WNW-striking, upright folds.

The sharp increase of metamorphic grade across the shear zone contrasts to the gradually increasing grade observed along the southern margin of the western Tauern Window. These features are similar but symmetrically opposite to the central Alps, where the sharpest metamorphic gradient and vertical displacement are localized along the southern side of the Lepontine dome (Fig. 1a).

Although we reject the idea that the SEMP Fault continuously splays into the three major shear zones of the western Tauern Window (the Ahorn, Greiner and Ahrntal shear zones), these three shear zones were probably coeval and belonged to the same sinistral system of the SEMP Fault. The en-echelon structure of these shear zones (Fig. 1b) and their parallelism to the upright folds suggest that the entire western Tauern Window may be regarded as a restraining bend connecting the sinistral displacements of the Giudicarie Fault System with the sinistral displacements of the SEMP Fault. Laboratory experiments (Ratschbacher *et al.* 1991*a*, EXP 1–23; Rosenberg *et al.* 2004; Rosenberg *et al.* 2007) show that the strike of the SEMP Fault may have been approximately NE, as the fault nucleated, i.e. much closer to the orientation of the Giudicarie Fault System. Subsequent deformation rotated the SEMP Fault into the present ENE strike, whereas the Giudicarie Fault, which marks the boundary of a nearly rigid indenter, maintained its initial orientation.

Due to its vertical orientation, this mylonitic belt was not imaged as a reflector along the recent TRANSALP seismic line, hence it was not shown in the geological interpretations of the seismic lines (e.g. Lüschen *et al.* 2004, 2006; Schmid *et al.* 2004). One exception is the interpretation of Ortner *et al.* (2006), who associated the northern termination of several gently south-dipping reflectors to two steep faults with south-side-up displacement, bounding the upper Schieferhülle. Our field data indicate that the Ahorn shear zone should be included in the cross-sections of the western Tauern Window, as a wide (2 km) subvertical structure, mainly located within the northern boundary of the Zentral Gneiss.

Field work has been supported by the Deutsche Forschungsgemeinschaft (Ro 2177/4-1). The high quality of the thin sections of W. Michaelis is much appreciated. Lothar Ratschbacher was extremely helpful, providing literature and suggesting localities where one could or could not possibly follow the ductile terminations of the SEMP Fault. We acknowledge discussions with Jochen Babist and Konrad Hammerschmidt who shared with us their ideas and field observations. Jane Selverstone and Hugo Ortner provided very constructive reviews of the manuscript. Oliver Kettler collected some of the structural data in Zillergrund. C. R. is indebted to Stefan Schmid for an excellent training in structural geology.

References

Barnes, J. D., Selverstone, J. & Sharp, Z. D. 2004. Interactions between serpentinite devolatilization, metasomatism and strike-slip strain localization during deep-crustal shearing in the Eastern Alps. *Journal of Metamorphic Geology*, **22**, 283–300.

Behrmann, J. H. 1988. Crustal-scale extension in a convergent orogen: the Sterzing-Steinach mylonite zone in the Eastern Alps. *Geodynamica Acta*, **2**, 63–73.

Behrmann, J. H. 1990. Zur Kinematik der Kontinentalkollision in den Ostalpen. *Geotektonische Forschungen*, **76**, 1–180.

Behrmann, J. & Frisch, W. 1990. Sinistral ductile shearing associated with metamorphic decompression in the Tauern Window, Eastern Alps. *Jahrbuch der Geologischen Bundesanstalt*, **133**, 135–146.

Borsi, S., Del Moro, A., Sassi, F. P., Zanferrari, A. & Zirpoli, G. 1978. New geopetrologic and radometric data on the alpine history of the austridic continental marigin south of the Tauern Window (Eastern Alps). *Consiglio Nazionale della Ricerca*, **32**, 3–17.

Burkhard, M. 1993. Calcite twins, their geometry, appearance and significance as stress-strain markers and indicators of tectonic regime: a review. *Journal of Structural Geology*, **15**, 351–368.

Christensen, J. N., Selverstone, J., Rosenfeld, J. L. & dePaolo, D. J. 1994. Correlation by Rb-Sr geochronology of garnet growth histories from different structural levels within the Tauern Window, Eastern Alps. *Contributions to Mineralogy and Petrology*, **118**, 1–12.

Cole, J. N., Hacker, B. R., Ratschbacher, L., Dolan, J. F., Seward, G., Frost, E. & Frank, W. 2007. Localized ductile shear below the seismogenic zone: structural analysis of the exhumed SEMP strike-slip fault, Austrian Alps. *Journal of Geophysical Research*, **112**, doi: 10.1029/2007JB004975.

De Vecchi, G. & Baggio, P. 1982. The Pennine zone of the Vizze region, in the Western Tauern Window (Italian Eastern Alps). *Bollettino della Società Geologica Italiana*, **101**, 89–116.

Decker, K., Peresson, H. & Faupl, P. 1994. Die miocäne Tektonik der östlichen Kalkaplen: Kinematik, Paläospannungen und Deformationsaufteilung während der 'lateralen Extrusion' der Zentralalpen. *Jahrbuch der Geologischen Bundesanstalt*, **137**, 5–18.

Fitz Gerald, J. D. & Stünitz, H. 1993, Deformation of granitoids at low metamorphic grades. I. Reactions and grainsize reduction. *Tectonophysics*, **221**, 269–297.

Frisch, W., Kuhlemann, A., Dunkl, I. & Brügel, A. 1998. Palinspastic reconstruction and topographic evolution of the Eastern Alps during late Tertiary tectonic extrusion. *Tectonophysics*, **297**, 1–15.

Frisch, W., Brügel, A. J., Dunkl, I., Kuhlemann, J. & Satir, M. 1999. Post-collisional large-scale extension and mountain uplift in the Eastern Alps. *Memorie di Scienze Geologiche (Padova)*, **51**, 3–23.

Frisch, W., Dunkl, I. & Kuhlemann, J. 2000. Post-collisional orogen-parallel large-scale extension in the Eastern Alps. *Tectonophysics*, **327**, 239–265.

Fry, N. 1979. Random point distributions and strain measurement in rocks. *Tectonophysics*, **60**, 89–105.

Fügenschuh, B., Seward, D. & Mantckelow, N. 1997. Exhumation in a convergent orogen: the western Tauern Window. *Terra Nova*, **9**, 213–217.

Handy, M. R. 1990. The solid-state flow of polymineralic rocks. *Journal of Geophysical Research*, **96**, 8647–8661.

Handy, M. R., Babist, J., Wagner, R., Rosenberg, C. L., Konrad, M. 2005. Decoupling and its relation to strain partitioning in continental lithosphere: insight from the Periadriatic fault system (European Alps). *In*: Gapais, D., Brun, J. P. & Cobbold, P. R. (eds) *Deformation Mechanisms, Rheology and Tectonics: from Minerals to the Lithosphere*. Geological Society of London, Special Publication, **243**, 249–276.

Hirth, G. & Tullis, J. 1992. Dislocation creep regimes in quartz aggregates. *Journal of Structural Geology*, **14**, 145–159.

Hörnes, S. & Friedrichsen, H. 1978. Oxygen isotope studies of the Austroalpine and Pennine units of the eastern Alps. *In*: Cloos, H., Roeder, D. & Schmidt, K. (eds) *Alps, Appennines, and Hellenides.* Inter-Union Committee on geodynamics Science Report, **38**, 127–131.

Inger, S. & Cliff, R. A. 1994. Timing of metamorphism in the Tauern Window, Eastern Alps: Rb-Sr ages and fabric formation. *Journal of Metamorphic Geology* **12**, 695–707.

Kleinschrodt, R. 1987. Quarzkorngefügeanalyse im Altkristallin südlich des westlichen Tauernfensters (Südtirol/Italien). Erlanger geologische Abhandlungen, **114**, 1–82.

Kupferschmied, M. 1993. Structural studies in the Western Habach Group (Tauern Window, Salzburg, Austria). *Abhandlungen der Geologische Bundesanstalt*, **49**, 67–78.

Kurz, W. & Neubauer, F. 1996. Deformation partitioning during updoming of the Sonnblick area in the Tauern Window (Eastern Alps, Austria). *Journal of Structural Geology*, **18**, 1327–1343.

Kurz, W., Unzog, W., Neubauer, F. & Genser, J. 2001. Evolution of quartz microstructures and textures during polyphase deformation within the Tauern Window (Eastern Alps). *International Journal of Earth Sciences*, **90**, 361–378.

Lammerer, B. 1988. Thrust-regime and transpression-regime tectonics in the Tauern Window (Eastern Alps). *Geologische Rundschau*, **77**, 143–156.

Lammerer, B. & Weger, M. 1998. Footwall uplift in an orogenic wedge: the Tauern Window in the Eastern Alps of Europe. *Tectonophysics*, **285**, 213–230.

Linzer, H.-G., Moser, F., Nemes, F., Ratschbacher, L. & Sperner, B. 1997. Build-up and dismembering of a classical fold-thrust belt: from non-cylindircal stacking to lateral extrusion in the eastern Northern Calcareous Alps. *Tectonophysics*, **272**, 97– 124.

Linzer, H.-G., Decker, K., Peresson, H., Dell' Mour, R. & Frisch, W. 2002, Balancing orogenic float of the Eastern Alps. *Tectonophysics*, **354**, 211–237.

Lüschen, E., Lammerer, B., Gebrande, H., Millhan, K. Nicolich, R. & Transalp Working Group 2004. Orogenic structure of the Eastern Alps, Europe from TRANSALP deep seismic reflection profiling. *Tectonophysics*, **388**, 85–102.

Lüschen, E., Borrini, D., Gebrande, H., Lammerer, B., Millahn, K., Neubauer, F. & Nicolich, R. 2006. TRANSALP—deep crustal Vibroseis and explosive seismic profiling in the Eastern Alps. *Tectonophysics*, **414**, 9–38.

Mancktelow, N. S., Stöckli, D. F., Grollimund, B. *et al.* 2001. The DAV and the Periadriatic fault system in the Eastern Alps south of the Tauern Window. *International Journal of Earth Sciences*, **90**, 593–622.

Miller, H., Ledoux, H., Brinkmeier, I. & Beil, F. 1984. Der Nordwestrand des Tauernfensters-stratigraphische Zusammenhänge und tektonische Grenzen. *Zeitschrift der deutschen geologischen Gesellschaft*, **135**, 627–644.

Most, P., Dunkl, I. & Frisch, W. 2003. Fission track tomography of the Tauern Window along the TRANSALP profile. *Memorie di Scienze Geologiche, Padova*, **54** (special vol.), 225–226.

Norris, J., Oxburgh, E. R., Cliff, R. A. & Wright, R. C. 1971. Structural, Metamorphic, and Geochronological Studies in the Reisseck and Southern Ankogel Groups, the Eastern Alps, Part IV, Structure. *Jahrbuch der geologischen Bundesanstalt*, **114**, 198–234.

Ortner, H. & Stingl, V. 2001. Facies and basin development of the Oligocene in the lower Inn Valley, Tyrol Bavaria. *In*: Piller, W. E. & Rasser, M. W. (eds) Palaeogene of the Eastern Alps. *Österreichische Akademie der Wissenschaften Schriftenreiche der Erdwissenschaftlichen Kommissionen*, **14**, 153–196.

Ortner, H., Reiter, F. & Brandner, R. 2003. Kinematics of the Inntal shear zone and its relation to other major faults crossing the northern TRANSALP seismic section. *Memorie di Scienze Geologiche, Padova*, **54**, 189–192.

Ortner, H., Reiter, F. & Brandner, R. 2006. Kinematics of the Inntal shear zone–sub-Tauern ramp fault system and the interpretation of the TRANSALP seismic section, Eastern Alps, Austria. *Tectonophysics*, **414**, 241–258.

Peresson, H. & Decker, K. 1997. Far-field effects of late Miocene subduction in the Eastern Carpathians: E-W compression and inversion of structures in the Alpine-Carpathian-Pannonian region. *Tectonics*, **16**, 38–56.

Ratschbacher, L., Merle, O., Davy, P. & Cobbold, P. 1991*a*. Lateral extrusion in the Eastern Alps, Part 1: Boundary conditions and experiments scaled for gravity. *Tectonics*, **10**, 245–256.

Ratschbacher, L., Frisch, W. & Linzer, H.-G. 1991*b*. Lateral extrusion in the Eastern Alps: Part II. Structural analysis. *Tectonics*, **10**, 257–271.

Reicherter, K., Fimmel, R. & Frisch, W. 1993. Sinistral strike-slip faults in the Central Tauern Window (Eastern Alps, Austria). A short note. *Jahrbuch der Geologischen Bundesanstalt*, **136**, 495–502.

Reinecker, J. & Lehnhardt, W. A. 1999. Present-day stress field and deformation in eastern Austria. *International Journal of Earth Sciences*, **88**, 532–550.

Robin, P.-Y. F. & Cruden, A. R. 1994. Strain and vorticity patterns in ideally ductile transpression zones. *Journal of Structural Geology*, **16**, 447–466.

Rosenberg, C. L. & Stünitz, H. 2003. Deformation and recrystallization of plagioclase along a temperature gradient. The example of the Bergell tonalite. *Journal of Structural Geology*, **25**, 391–410.

Rosenberg, C. L., Brun, J.-P. & Gapais, D. 2004. Indentation model of the Eastern Alps and the origin of the Tauern Window. *Geology*, **32**, 997–1000.

Rosenberg, C. L., Brun, J.-P., Cagnard, F. & Gapais, D. 2007. Oblique indentation in the Eastern Alps: insights from laboratory experiments. *Tectonics*, **26**, TC2003; doi: 10.1029/2006TC001960.

Sander, B. 1920. Geologische Studien am Westende der Hohen Tauern. II Bericht. *Jahrbuch der Geologische Staatsanstalt*, **70**, 273–296.

Schmid, S. M., Fügenschuh, B., Kissling, E. & Schuster, R. 2004. Tectonic map and overall architecture of the Alpine orogen. *Eclogae Geologicae Helvetiae*, **97**, 93–117.

Selverstone, J. 1985. Petrologic constraints on imbrication, metamorphism, and uplift in the Tauern Window, Eastern Alps. *Tectonics*, **4**, 687–704.

Steffen, K. J., Selverstone, J. & Brearley, A. 2001. Episodic weakening and strengthening during synmetamorphic deformation of a deep crustal shear zone in the Alps. *In*: Holdsworth, R., Strachan, R., Magloughlin, J. & Knipe, R. (eds) *The Nature and Tectonic Significance of Fault Zone Weakening*, Geological Society of London, Special Publication, **186**, 141–156.

Steffen, K. J. & Selverstone, J. 2006. Retrieval of P-T information from shear zones: thermobarometric consequences of changes in plagioclase deformation mechanisms. *Contributions to Mineralogy and Petrology*, **151**, 600–614.

Steininger, F., Rögl, F., Hochuli, P. & Müller, C. 1989. Lignite deposition and marine cycles. The Austrian Tertiary lignite deposits. A case history. *Sitzungsbericht der Akademie der Wissenschaften, Wien, mathematisch- naturwissenschaftliche Klasse*, **197**, 309–332.

Stipp, M., Stünitz, H., Heilbronner, R. & Schmid, S. M. 2002. The eastern Tonale fault zone: a 'natural laboratory' for crystal plastic deformation of quartz over a temperature range from 250 to 700 °C. *Journal of Structural Geology*, **24**, 1861–1884.

Stipp, M., Tullis, J. & Behrens, H. 2006. Effect of water on the dilocation creep microstructure and flow stress of quartz and implications for the recrystallized grain size piezometer. *Journal of Geophysical Research*, **111**, B04201; doi: 10.1029/2005JB003852.

Twiss, R. J. & Moores, E. M. 1992. *Structural Geology*. W. H. Freeman & Co.

Wagner, R., Rosenberg, C. L., Handy, M. R., Möbus, C. & Albertz, M. 2006. Fracture-driven intrusion and upwelling of a mid-crustal pluton fed from a transpressive shear zone: the Rieserferner pluton (Eastern Alps). *Geological Society of America, Bulletin*, **118**, 219–237; doi: 10.1130/B25842.1.

Wang, X. & Neubauer, F. 1998. Orogen-parallel strike-slip faults bordering metamorphic core complexes: the Salzach-Enns fault zone in the Eastern Alps. *Journal of Structural Geology*, **20**, 799–818.